Available online at www.sciencedirect.com
ScienceDirect
Acta Materialia 58 (2010) 3281–3294
Acta MATERIALIA
www.elsevier.com/locate/actamat

Formation mechanisms of cyclic saturation dislocation patterns in [0 0 1], [0 1 1] and [$\bar{1}$ 1 1] copper single crystals

P. Li *, S.X. Li, Z.G. Wang, Z.F. Zhang *

Shenyang National Laboratory for Materials Science, Institute of Metal Research, Chinese Academy of Sciences, 72 Wenhua Road, 110016 Shenyang, China

Received 24 November 2009; received in revised form 1 February 2010; accepted 2 February 2010
Available online 5 March 2010

Abstract

This work reveals the formation mechanisms of saturation dislocation patterns in three typical multiple-slip oriented [0 0 1], [0 1 1] and [$\bar{1}$ 1 1] copper single crystals. Compared with the single-slip oriented copper single crystals, the three multiple-slip oriented ones show very different dislocation patterns. It was found that the dislocation patterns in cyclically saturated copper single crystals are the Labyrinth structure for [0 0 1], wall structure for [0 1 1] and cell structure for [$\bar{1}$ 1 1], respectively. Based on a two-phase structure consisting of persistent slip bands and veins for single-slip orientation, the formation mechanisms of the dislocation patterns in multiple-slip oriented crystals are proposed as follows: the formation of the complex dislocation patterns depends on the activating slip system. The easy operation of the critical secondary slip system will contribute to the formation of the Labyrinth structure. The activation of the coplanar secondary slip system will be beneficial to formation of the cell structure. If no secondary slip system is activated, the wall structure is more prone to appear. Finally, the intrinsic relationship between various dislocation patterns and face centered cubic crystal structure was established.

Keywords: Orientation effect; Cyclic deformation; Copper single crystals; Dislocation patterns

1. Introduction

The "persistent" phenomenon of fatigue-induced slip bands was defined for the first time in 1956 by Thompson et al. [1] in their study of the nature and properties of slip bands in fatigued copper mono- and poly-crystals. They found that these "persistent slip bands" (PSB) reappeared at the old sites when the specimen was fatigued again after the previously formed slip bands had been polished away. Later, these PSB were confirmed convincingly by Laufer and Roberts [2] to be not merely a surface but a bulk phenomenon. These authors discovered that the dislocation patterns in PSB were distinct from those of the surrounding so-called matrix and consisted of the so-called wall or ladder structure. Thereafter, Winter [3] in 1974 and Finney and Laird [4] in 1975 successively proposed a two-phase model to explain the cyclic saturation dislocation structures. Based on these early studies, Mughrabi [5] established the famous cyclic stress–strain (CSS) curve of copper single crystals oriented for single slip and found that the CSS curve clearly demonstrated three regions, A, B and C. For copper crystals cycled in region A, the matrix veins form, and the larger the applied strain amplitude, the higher the saturation stress. The onset of region B is marked by the formation of the first PSB [6–9]. As the strain amplitude increases in region B, the volume fraction of the PSB increases accordingly [3,4,10,11], and the CSS curve shows a plateau behavior with a strain-independent saturation stress of ~28 MPa. With further increasing strain amplitude up to region C, the saturation stress increases again, and the dislocation structure is characterized by dislocation cells or Labyrinth structure. Soon after, Cheng and Laird [12] found that, for most single-slip oriented copper single crystals, their saturation stress amplitudes at room temperature are in the range 28–30 MPa.

* Corresponding authors. Tel.: +86 24 23971043; fax: +86 24 23891320.
E-mail addresses: pli@imr.ac.cn (P. Li), zhfzhang@imr.ac.cn (Z.F. Zhang).

1359-6454/$36.00
doi:10.1016/j.actamat.2010.02.002

Based on single-slip oriented copper single crystals, different double-slip even multiple-slip oriented ones were investigated in succession. Jin and Winter [13–16] systematically studied the cyclic deformation behavior of three copper single crystals with [0 1 2], [$\bar{1}$ 1 2] and [$\bar{1}$ 2 2] double-slip orientations. They found that different regions in the stereographic triangle corresponded to different dislocation interaction models, which resulted in different cyclic hardening rates, saturation stresses and dislocation patterns. As for multiple-slip orientations, Lepisto et al. [17–19] and Gong et al. [20,21] investigated the cyclic deformation behavior of [$\bar{1}$ 1 1] and [0 0 1] copper single crystals, respectively. The results indicated that the CSS curves in both multiple-slip oriented copper single crystals did not present any plateau behavior. Furthermore, they found that the dislocation patterns of [$\bar{1}$ 1 1] and [0 0 1] copper single crystals after cyclic saturation consisted mainly of cell and Labyrinth structure, respectively. Later, Li et al. [22] investigated the cyclic hardening rates, CSS curves and corresponding dislocation patterns of [0 1 1] copper single crystals. They found that the cyclic deformation behavior of [0 1 1] copper single crystals is quite different from those of [$\bar{1}$ 1 1] and [0 0 1] copper single crystals. The CSS curve of [0 1 1] single crystal shows clear plateau behavior, which is similar to the single-slip oriented copper single crystals. However, the difference is that deformation band II (DBII) appears more easily on the surface of cyclically saturated [0 1 1] copper single crystal. In general, two types of DB, namely DBI and DBII, have been identified in fatigued copper single crystals, where DBI is approximately parallel to the primary slip plane, while DBII makes a certain angle with the primary slip plane. Based on systematic investigations on the fatigue behavior of copper single crystals with double- and multiple-slip orientations, Li et al. [23–26] gave a clear and comprehensive summary on the orientation effect of copper single crystals, which can be briefly introduced as follows (see Fig. 1a): for the coplanar double-slip oriented copper single crystals located on the 0 1 1/$\bar{1}$ 1 1 side of the stereographic triangle, the CSS curves transform from a clear plateau region in the [0 1 1] crystal to no plateau region in the [$\bar{1}$ 1 1] crystal. On the 0 0 1/0 1 1 side, the CSS curves exhibit a gradually narrower plateau region from [0 1 1] to [0 0 1] crystal. On the 0 0 1/$\bar{1}$ 1 1 side of the stereographic triangle, the CSS curve of the [$\bar{1}$ 1 2] copper single crystal exhibited a clear plateau region, which is shorter than that of the single-slip crystals, although the saturation resolved shear stress amplitudes are nearly the same. However, the CSS curve of [$\bar{1}$ 1 7] crystal did not show any plateau region, which is similar to that of [$\bar{2}$ 2 3] and [$\bar{1}$ 1 1] single crystals. Corresponding to the CSS curve, the dislocation pattern of differently oriented copper single crystals is different, with distinct characteristics. Fig. 1b shows that the PSB ladder structure appears in copper single crystals with the single-, [$\bar{1}$ 1 2] double- and [0 1 1] multiple-slip orientations. As the orientation of copper single crystals changes from [0 1 1] to [0 0 1] in the stereographic triangle, the corresponding dislocation patterns vary from PSB ladders to Labyrinth structure. When the orientation changes from [0 1 1] to [$\bar{1}$ 1 1], PSB ladders are gradually converted into the cell-like structure.

In parallel with the studies on copper single crystals, it is found that the orientation has a similar influence on the cyclic deformation behavior of nickel single crystals. The results from Bretschneider et al. [27] show that the CSS curve of nickel single crystals oriented for single slip is consistent with those of copper single crystals, apart from a

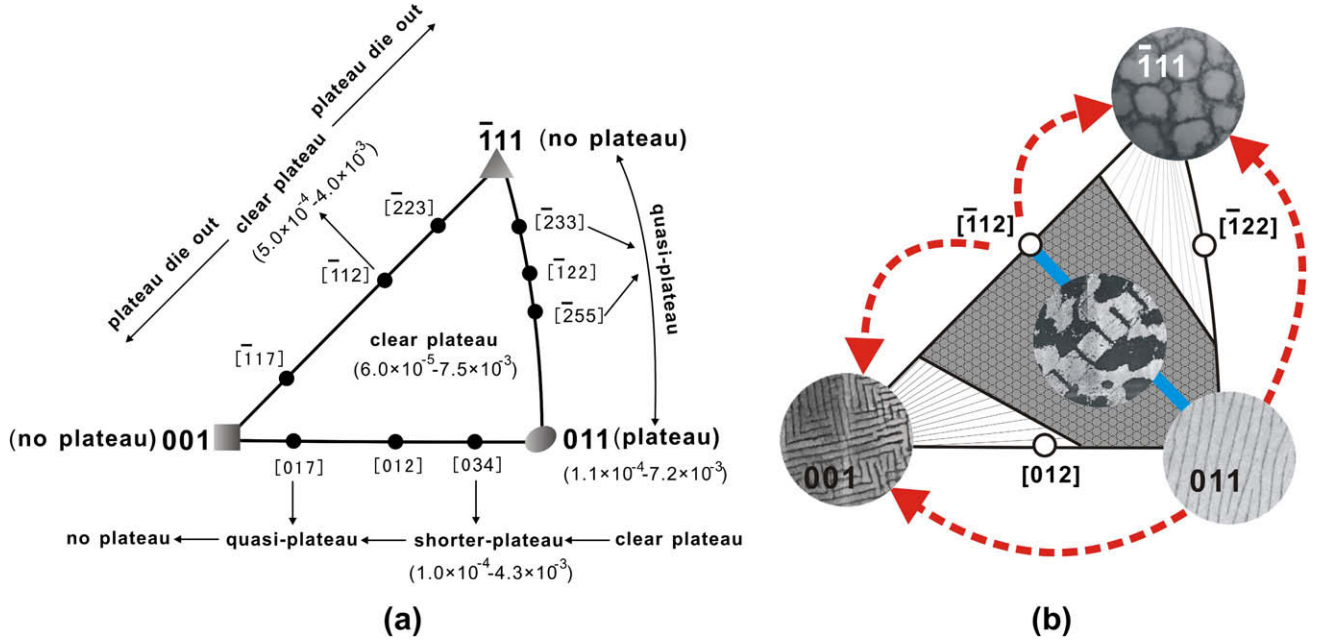

Fig. 1. Effect of orientation on the cyclic deformation and dislocation patterns of fcc single crystals: (a) effect of orientation on CSS curves of copper single crystals [23] and (b) general principle of the effect of orientation on dislocation patterns [35].

higher saturation resolved shear stress (50–52 MPa). Based on the comparison with the results from Bretschneider et al. [27] and Kahle [28], Buque et al. [29,30] systematically summarized the CSS curves and the classical dislocation configurations of nickel single crystals with different orientations and found that there are apparent plateau regions and classical PSB ladders in $[\bar{1}\,4\,9]$ and [0 1 1] nickel single crystals. In contrast, a Labyrinth structure appears in the [0 0 1] nickel single crystal, and a cell-wall structure forms in the $[\bar{1}\,1\,1]$ nickel single crystal. As the orientation changes from $[\bar{1}\,4\,9]$ or [0 1 1] to [0 0 1], more to $[\bar{1}\,1\,1]$, the CSS curve of nickel single crystals shows a continuous elevation or inclination as a rule.

In addition to copper and nickel, silver is another typical face centered cubic (fcc) metal. Investigation into the cyclic deformation behavior of silver single crystals is still rare. Sastry et al. [31] investigated the saturation dislocation structure of $[\bar{1}\,2\,8]$ silver single crystals cyclically deformed over the strain range $2.5 \times 10^{-3} < \gamma_{pl} < 2.5 \times 10^{-2}$. Mughrabi et al. [32] systematically studied the cyclic deformation behavior of silver single crystals and compared them with those of copper and nickel single crystals. They concluded that, for the three typical fcc metals, the characteristic thresholds of the stress required for the formation of the first PSB, expressed as τ_{PSB}/G, exist and have similar values of $(6.5 \pm 0.5) \times 10^{-4}$. Recently, the present authors [33–35] further studied the CSS curves, surface slip morphologies and dislocation patterns of differently oriented silver single crystals. After the results of copper and nickel single crystals with similar orientation are compared, it can be concluded that the orientation effects on cyclic deformation behavior follow a general principle: the orientation-dependent dislocation configurations can be divided into three regions in the stereographic triangle, including the central region, [0 0 1] and $[\bar{1}\,1\,1]$ regions (see Fig. 1b). When the plastic shear strain amplitude γ_{pl} resolved on the primary slip system is close to 6×10^{-5} for the formation of the first PSB, the dislocation patterns in the central region are characterized by the PSB ladder or wall structure. In the [0 0 1] region, the dislocation patterns consist of the Labyrinth structure. And in the $[\bar{1}\,1\,1]$ region, the cell structure is more easily found. The dislocation structures and plateau behavior in the three regions have their respective characteristics, so the investigation of the orientation effects can be simplified to an investigation of the three multiple-slip oriented fcc single crystals. Naturally, another question will be asked: What are the intrinsic formation mechanisms of different dislocation patterns in the three multiple-slip oriented single crystals? In other words, what kind of role does the orientation play during cyclic deformation of fcc single crystals? To reveal the intrinsic relationship between the dislocation patterns and the orientation, three typical multiple-slip oriented copper single crystals were selected as model materials, and further discussion is made by systematically investigating the formation of their dislocation patterns.

2. Experimental procedures

Three bulk single crystals with specific orientations [0 0 1], [0 1 1] and $[\bar{1}\,1\,1]$ were grown from electrolytic copper of 99.999% purity by the Bridgman method in a horizontal furnace. Later, fatigue specimens with $7 \times 5 \times 16$ mm gauge section and 54 mm total length were made using an electro-spark cutting machine.

The loading axes of the specimens are parallel to the [0 0 1], [0 1 1] and $[\bar{1}\,1\,1]$ orientations, respectively. The crystal orientation was determined by the electron backscattering diffraction (EBSD) technique with accuracy within $\pm 2^\circ$ in a Cambridge S360 scanning electron microscope. Cyclic deformation was performed under symmetric push–pull loading at room temperature in air, using a Shimadzu servohydraulic testing machine. A triangular waveform signal with frequency 0.5 Hz was used for total strain control with the limitation of plastic strain. Plastic strain resolution and control precision were better than 10^{-5}. The peak loads in tension and compression and the hysteresis loops were recorded automatically by computer until cyclic saturation. After the fatigue tests, all the fatigued specimens were electro-polished carefully and, subsequently, the dislocation configurations beneath the surface were carefully observed by the electron channeling contrast (ECC) technique in a Cambridge S360 scanning electron microscope. Such ECC images are similar in appearance to transmission electron micrographs, albeit with a lower image resolution [36–39]. However, the ECC technique in the scanning electron microscope has a great advantage in the observations of fatigued dislocation patterns in a larger area, especially near grain boundaries, deformation bands or fatigue cracks [40–43].

3. Results and discussion

3.1. CSS curves of copper single crystals with multiple-slip orientations

Table 1 lists in detail the fatigue testing conditions and experimental data for cyclic hardening and saturation stresses in three classical multiple-slip oriented copper single crystals, where γ_{pl} is the constant plastic shear strain amplitude, $\gamma_{pl,cum}$ ($\gamma_{pl,cum} = 4N\gamma_{pl}$, N is the number of cycles) is the cumulative plastic strain, τ_s is the saturation resolved shear stress, and τ_{max} is the maximum shear stress. In order to analyze these data more completely and objectively, the experimental results from other researchers are also added to Table 1 for comparison. The saturation stress of $[\bar{1}\,1\,1]$ copper single crystals should be especially emphasized because it is extremely difficult to complete fatigue test with this orientation, especially at high strain amplitudes. The cyclic hardening curve of $[\bar{1}\,1\,1]$ copper single crystals does not show the saturation behavior well. Therefore, Lepisto and Kettunen [18] decided to replace the saturation stress by the maximum (peak) stress in the CSS curve. Of course, this treatment will bring some error,

Table 1
Fatigue testing conditions and data for multiple-slip-oriented copper single crystals; partial data for [0 0 1], [0 1 1] and [$\bar{1}$ 1 1] copper single crystals, quoted from Gong et al. [20], Li et al. [22] and Lepisto and Kettunen [18], respectively.

Orientation	Specimen no.	γ_{pl}	Cycles	$\gamma_{pl.cum}$	τ_s (MPa)	τ_{max} (MPa)	Investigators
[0 0 1]	1	1.22×10^{-4}	20,000	9.76	23.4	23.9	Present result
	2	2.5×10^{-4}	10,000	10	25.9	26.4	
	3	6.1×10^{-4}	5000	12.2	29.8	30.5	
	4	1.0×10^{-3}	2000	8	39	41.2	
	5	2.5×10^{-3}	2000	20	44	48.5	
	1	1.0×10^{-4}	75,000	30	20.3	20.3	Gong et al. [20]
	2	2.4×10^{-4}	32,610	31.3	26.7	26.7	
	3	4.8×10^{-4}	27,320	52.5	31.53	36.02	
	4	6.0×10^{-4}	34,480	82.7	36.16	39.54	
	5	7.2×10^{-4}	3110	9	38.62	42.26	
	6	1.8×10^{-3}	10,420	75	41.09	42.72	
	7	3.0×10^{-3}	3080	37	45.63	46.47	
[0 1 1]	1	1.22×10^{-4}	50,000	24.4	28.9	28.9	Present result
	2	6.1×10^{-4}	20,000	48.8	29.2	31.9	
	3	1.22×10^{-3}	10,000	48.8	29.5	29.5	
	4	2.5×10^{-3}	5000	50	29.1	29.1	
	5	7.35×10^{-3}	2000	58.8	33.5	36.4	
	1	1.1×10^{-4}	59,000	26	29.2	30.6	Li et al. [22]
	2	2.8×10^{-4}	32,800	36.7	29.3	33	
	3	7.3×10^{-4}	16,120	47.1	30.7	35.6	
	4	1.2×10^{-3}	11,220	53.9	29.6	34.1	
	5	2.5×10^{-3}	4600	46	29.5	30.1	
	6	3.3×10^{-3}	3320	43.8	29.9	30.4	
	7	5.0×10^{-3}	2800	56	28.8	32.2	
	8	7.2×10^{-3}	2000	57.6	30.9	35	
[$\bar{1}$ 1 1]	1	1.84×10^{-4}	20,000	14.72	32.6	32.6	Present result
	2	0.92×10^{-3}	5000	18.4	–	39.4	
	1	3.0×10^{-4}	15,300	18.4	–	36.2	Lepisto and
	2	4.0×10^{-4}	8120	13	–	41.5	Kettunen [18]
	3	7.0×10^{-4}	1842	5.2	–	39.6	
	4	1.0×10^{-3}	555	2.2	–	41.9	
	5	1.4×10^{-3}	165	0.9	–	46.8	
	6	2.5×10^{-3}	122	1.2	–	60.9	

but could well reflect the change trend of shear stress with the increase in strain amplitude. This treatment method is followed in the present work.

Fig. 2 summarizes the CSS curves of the three multiple-slip oriented copper single crystals, among which [$\bar{1}$ 1 1] copper single crystal has the highest shear stress. From Fig. 2, the similarity and difference in the CSS curves between three multiple-slip orientations and single-slip ones can be clearly identified. In agreement with the same oriented nickel and silver single crystals [29,35], the CSS curve of [0 1 1] copper single crystal also shows obvious plateau behavior, except that the plateau stress is slightly higher than that of single-slip oriented copper single crystal. However, in [0 0 1] and [$\bar{1}$ 1 1] copper single crystals, there is no plateau region in their CSS curves (see Fig. 2). Their respective saturation stresses increase monotonically with increasing strain amplitudes. From Table 1 it can also be seen that the data from Gong et al. [20] and Li et al. [22] are very consistent with the data from the present [0 0 1] and [$\bar{1}$ 1 1] copper single crystals, which further strengthens understanding of the cyclic deformation characteristics in copper single crystals with different orientations.

The macroscopic deformation behavior is dominated by the microscopic dislocation patterns. For example, the appearance of the plateau region corresponds to the formation of PSB. Therefore, for the three typical multiple-slip oriented copper single crystals, various dislocation patterns are just the reason for the similarity and difference of the CSS curves. In the following, the formation mechanisms of different dislocation patterns will be discussed, taking into account the respective orientation effects.

3.2. Formation mechanism of Labyrinth structure in [0 0 1] single crystal

Fig. 3 presents the dislocation patterns of [0 0 1] copper single crystal cyclically deformed at different plastic strain amplitudes. When γ_{pl} is 1.22×10^{-4}, the dislocation patterns consist of vein structures (see Fig. 3a). But the vein in [0 0 1] copper single crystals shows some directivity, which is different from that of single-slip oriented crystals. However, similar to the single-slip oriented crystals, PSB ladder structures can also be seen in some local regions of [0 0 1] copper single crystal, as shown in Fig. 3b. How-

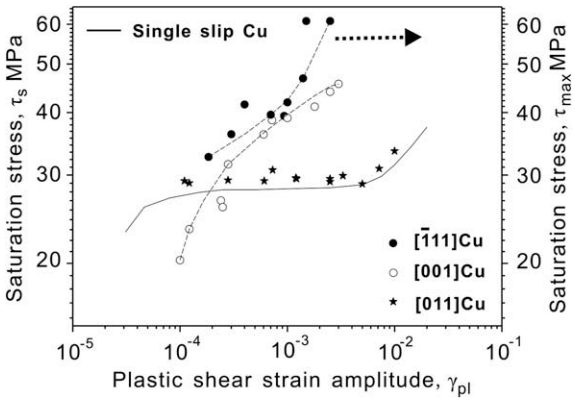

Fig. 2. Comparison of CSS curves among multiple-slip-oriented copper single crystals. Partial data quoted from Gong et al. [20], Li et al. [22] and Lepisto and Kettunen [18].

ever, these PSB ladders disappear very quickly at higher strain amplitudes. For example, at the plastic strain amplitude γ_{pl} of 2.5×10^{-4}, [0 0 1] copper single crystal is filled with the irregular Labyrinth structures (see Fig. 3c). The emergence of these Labyrinth-like structures broke the two-phase structure consisting of PSB and matrix veins. With increasing strain amplitudes, these dislocation structures will finally evolve into regular Labyrinth structures, as shown in Fig. 3d. In the (0 1 0) longitudinal section, regularly spaced thin walls parallel to (0 0 1) and (1 0 0) were found [15]. Both sets had the same spacing of ~0.50 μm. Their intersection with the (0 1 0) plane resulted in the Labyrinth structure. Meanwhile, Jin and Winter [44] found that the walls parallel to (0 0 1) were much more common than that parallel to (1 0 0). The same phenomenon can also be seen in Fig. 3d. The Labyrinth structure has its own distinctive features: two sets of mutual perpendicular walls. How do these walls form?

Fig. 4 indicates the position of the [0 0 1] orientation in the stereographic projection. The standard stereographic triangle corresponds to the region surrounded by 0 0 1–0 1 1–$\bar{1}$ 1 1. Actually, any triangle in the stereographic projection is equivalent, so the results obtained from any stereographic triangle have equivalence. It is known that [0 0 1] orientation has eight sets of equivalent slip systems with the same Schmid factor of 0.404, which can be activated simultaneously. However, a crystal with any orientation cannot strictly deform in accordance with the above analysis. Usually, the orientation of any crystal can be approximately regarded as single-slip orientation fallen in one of the stereographic triangles. Assuming, still in the triangle of 0 0 1–0 1 1–$\bar{1}$ 1 1, that the primary slip system (1 1 1)[$\bar{1}$ 0 1] was first operated, the more easily activated secondary slip systems are only conjugate and critical slip systems. In the previous study [35], it was learned that the conjugate-double-slip orientations do not affect the formation of the plateau behavior and the corresponding two-phase dislocation structure. Besides, Jin et al. [13,14] pointed out that conjugate dislocation reactions produced stable and non-slip Lomer–Cottrell dislocation locks. The reaction is so strong that the subsequent dislocation movement is obstructed. The obstruction made the dislocations in the different slip systems occupy clearly separated regions, in each of which a set of two-phase structure was formed. Therefore, the effect of the conjugate dislocation reaction on the formation of Labyrinth structure can be negligible. However, recent research [45] demonstrated that critical dislocation reactions produced sessile jogs, which also hindered the subsequent dislocation movement. But unlike dislocation locks, the reaction intensity of sessile jogs is weak. Thus, the dislocations belonging to the respective slip systems will overcome the resistance to keep the

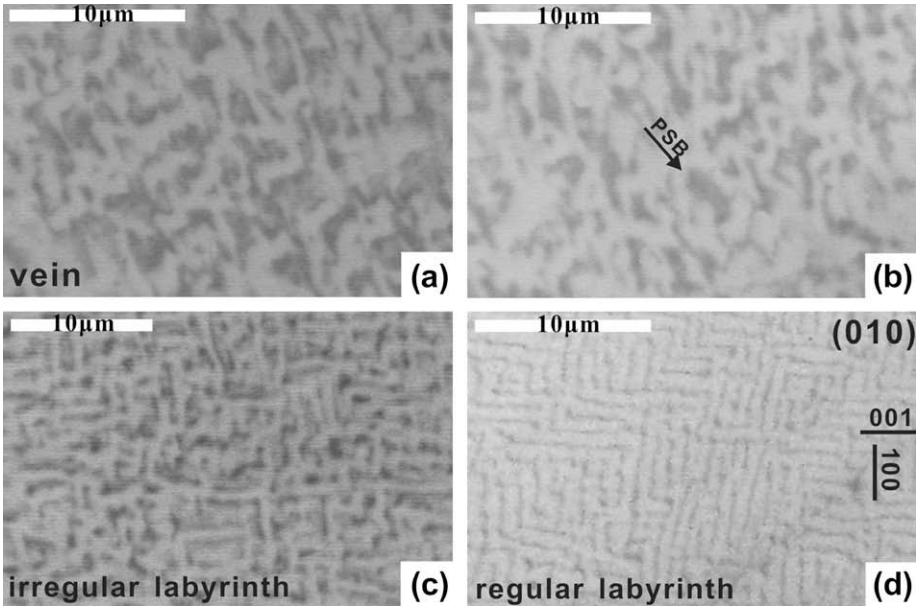

Fig. 3. Dislocation configurations of [0 0 1] copper single crystals at different plastic strain amplitudes: (a and b) $\gamma_{pl} = 1.22 \times 10^{-4}$; (c) $\gamma_{pl} = 2.5 \times 10^{-4}$; (d) $\gamma_{pl} = 2.5 \times 10^{-3}$. Viewed from (0 1 0) plane.

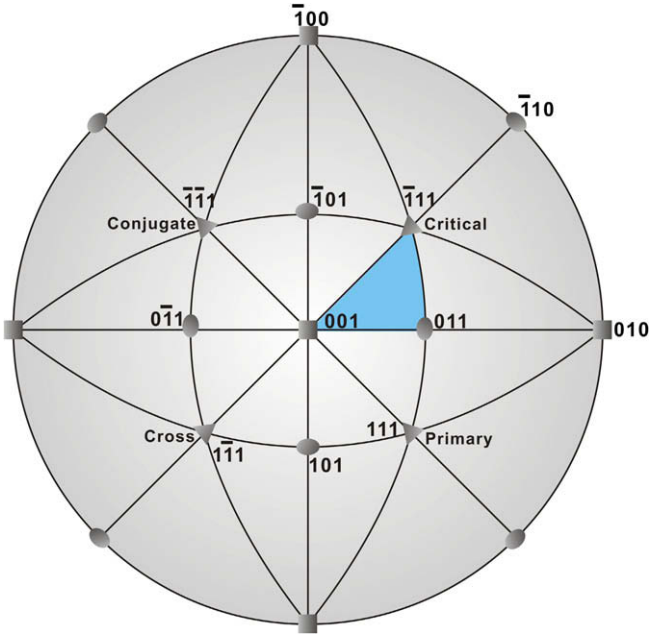

Fig. 4. Easily activated slip systems in [0 0 1] copper single crystals.

interaction with each other. They will not be strictly limited to their respective regions and affect each other in the process of the development. The formation of the Labyrinth structure results from this effect.

Now it is clear that the formation of Labyrinth structure is related to the activating critical slip system and how the Labyrinth forms by dislocation reactions. Fig. 5 illustrates the formation of Labyrinth structure [44]. The (0 1 0) plane is the best plane to observe the Labyrinth structure. On the (0 1 0) plane, two sets of PSB ladders belonging to the primary and critical second slip systems have formed, which accords with the movement and development of dislocations in their respective regions (see Fig. 5a). With cyclic deformation, the reaction between dislocations along $[\bar{1}\,0\,1]$ and [1 0 1] will take place, as shown in Fig. 5b. The result of the reactions can be expressed as:

$$\frac{1}{2}[\bar{1}\,0\,1]+\frac{1}{2}[1\,0\,1]=[0\,0\,1] \quad (1)$$

$$\frac{1}{2}[1\,0\,\bar{1}]+\frac{1}{2}[1\,0\,1]=[1\,0\,0] \quad (2)$$

From Fig. 4, it is well known that the slip directions of the primary and critical secondary slip systems are $[\bar{1}\,0\,1]$ and [1 0 1], respectively. The two slip directions correspond to the Burgers vectors of their respective dislocations. By summing the above vectors, new Burgers vectors can be identified as [0 0 1] and [1 0 0] and the corresponding shear planes are (1 0 0) and (0 0 1) planes (see Fig. 5b), respectively. Therefore, the shear systems corresponding to two sets of walls in the Labyrinth can be expressed as (1 0 0)[0 0 1] and (0 0 1)[1 0 0]. Their intersections with the (0 1 0) plane form the eventual Labyrinth structure. Nowadays, it should be clear that the activating of the critical secondary slip system and its interaction with the primary slip system are the basic processes for the formation of the Labyrinth structure in [0 0 1] crystals. However, why is (0 1 0) the best plane to observe the Labyrinth structure? It can be seen from Fig. 4 that, among all the orientations, the normal direction of only the (0 1 0) plane is perpendic-

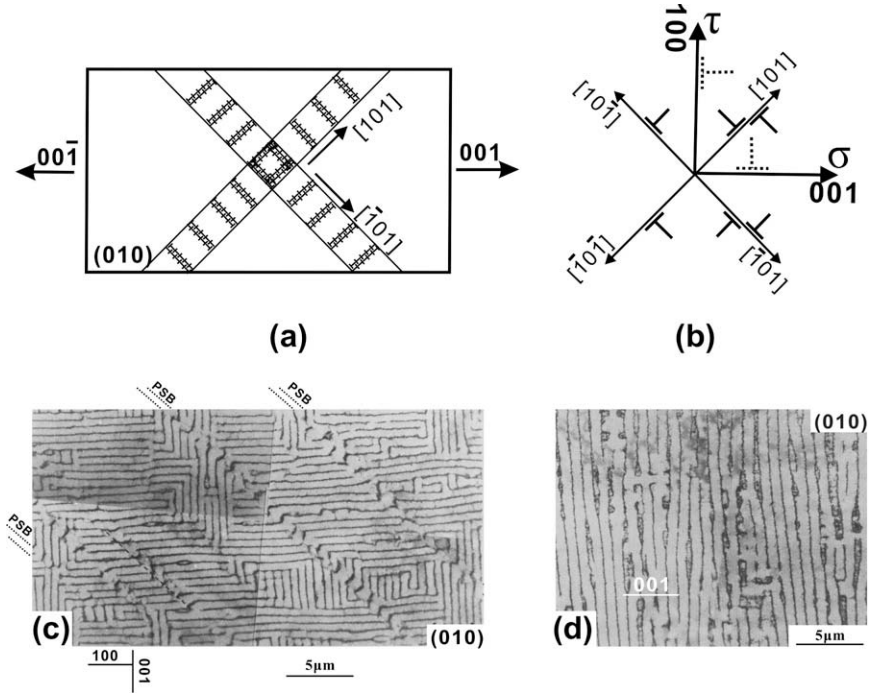

Fig. 5. Labyrinth-wall structure of [0 0 1] fcc single crystal: (a and b) illustration of formation of Labyrinth structure; (c) walls perpendicular to loading axis; (d) Labyrinth structure of (0 0 1) and (1 0 0) walls. (c and d) quoted from Jin and Winter [44].

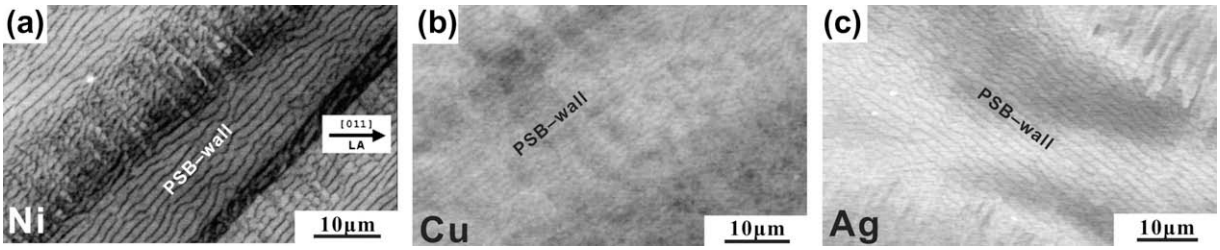

Fig. 6. Dislocation configurations of [0 1 1] nickel, copper and silver single crystals: (a) nickel single crystal cycled at $\gamma_{pl} = 6.1 \times 10^{-4}$, viewed from $(\bar{1}\,1\,\bar{1})$ plane, quoted from Buque [29]; (b) copper single crystal cycled at $\gamma_{pl} = 1.22 \times 10^{-3}$, viewed from $(\bar{1}\,2\,\bar{2})$ plane; (c) silver single crystal cycled at $\gamma_{pl} = 6.1 \times 10^{-4}$, viewed from $(2\,\bar{1}\,1)$ plane.

ular to the two slip directions of $[\bar{1}\,0\,1]$ and $[1\,0\,1]$ simultaneously. Jin and Winter [44] further determined that walls parallel to (0 0 1) were much more common than (1 0 0) walls (see Fig. 5c), and some specimens even showed (0 0 1) walls exclusively (see Fig. 5d). The reason for the prevalence of (0 0 1) walls is still unclear and further research will be necessary.

3.3. Formation mechanism of wall structure in [0 1 1] single crystal

Fig. 6 presents the dislocation patterns of [0 1 1] copper, nickel and silver single crystals. Apart from the PSB-vein structure, the wall structure is also often seen. The common feature in the three kinds of single crystals is the appearance of DBII, whose habit planes are the same and close to $(\bar{1}\,0\,1)$ [46]. In other words, the habit plane of dislocation walls in DBII is also close to $(\bar{1}\,0\,1)$. How do these wall structures in DBII form? And why is the wall structure made up of DBII easier to be seen in [0 1 1] fcc single crystals?

The primary slip system in fcc crystals is $(1\,1\,1)[\bar{1}\,0\,1]$, and the habit system of DBII is $(\bar{1}\,0\,1)[1\,1\,1]$ (see Fig. 7a), which manifests the conjugated relationship in crystallography between slip system and habit system. Based on the orientation relationship above (Fig. 7b), the resolved shear stress along the slip direction τ_a and that along the habit direction τ_b can be expressed as follows, respectively:

$$\tau_a = \sigma \cos\varphi \cos\phi = \Omega\sigma \tag{3}$$

$$\tau_b = \sigma \cos\phi \cos\varphi = \Omega\sigma \tag{4}$$

where ϕ is the interacting angle between the loading direction and the normal direction of the glide plane, φ is the interacting angle between the loading direction and the slip direction, ψ is the interacting angle between the loading direction and the normal direction of the best observation plane $(1\,\bar{2}\,1)$, and Ω is the Schmid factor. Comparing Eqs. (3) and (4), a basic judgment can be made that $\tau_{DBII} = \tau_b = -\tau_a = \tau_{SB}$. Under the same axial stress, $(1\,1\,1)[\bar{1}\,0\,1]$ and $(\bar{1}\,0\,1)[1\,1\,1]$ systems in fcc crystals have identical resolved shear stress. The reason why the [0 1 1] crystal is first to choose $(1\,1\,1)[\bar{1}\,0\,1]$ as the primary slip system is that the slip along the most close-packed plane and the most close-pack direction will encounter the smallest lattice resistance, which is still attributed to the effect of crystal structure. According to this idea, the formation of wall structures in DBII can be imagined as follows: under the action of the shear stress τ_a, the [0 1 1] crystal begins to glide along the slip plane. With constant cyclic loadings, the dislocations capture each other by continuous aggregation and evolution to form regular dislocation patterns: a PSB ladder structure. If the strain amplitude is further increased, a single PSB will not be able to carry the higher plastic deformation. Usually, the crystal makes adjustment by activating the secondary slip system, thereby the Labyrinth or cell structures appear in the crystal.

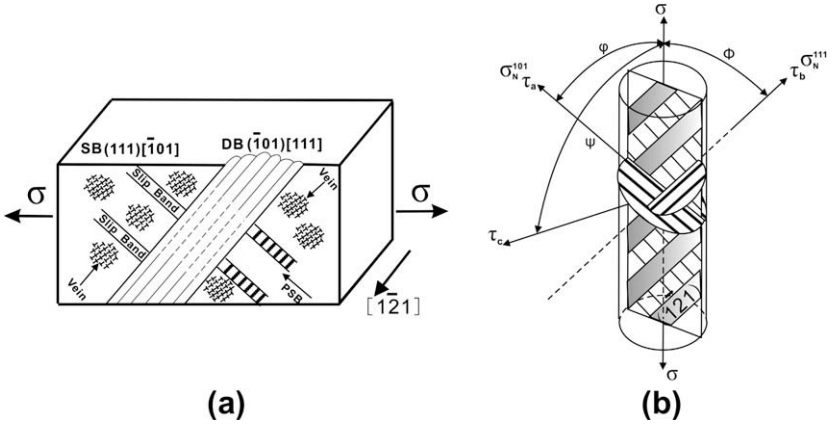

Fig. 7. Schematic map of the resolution axial stress: (a) habit planes of SB and DBII, respectively and (b) decomposition of the axial stress σ based on different habit planes.

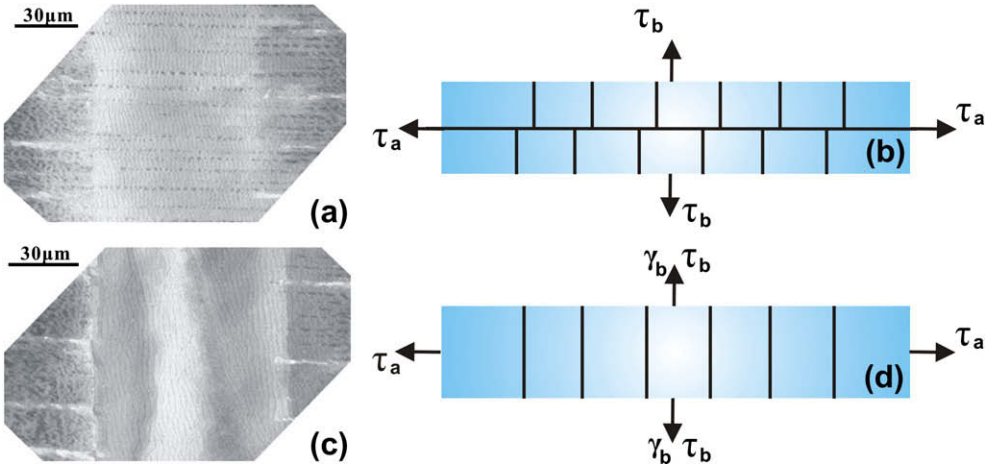

Fig. 8. Illustration maps of the formation of DBII: (a) developing DB; (b) PSB ladders in developing DB; (c) well-developed DB; (d) PSB walls in well-developed DB. (a and c) quoted from Zhang et al. [42].

But sometimes the secondary slip system is not easily activated or cannot be activated in time, especially in some local regions. In this case, the crystal will adopt another way to carry a greater plastic deformation, leading to the formation of DBII [42]. As shown in Fig. 8a, during the development of DBII the slip bands (SB) closely align, so the ladder structures in these SB move back and forth along the slip plane (see Fig. 8b). Under the action of the shear stress τ_b, there is always a moment for the PSB ladders to connect with each other to constitute the shear plane, as shown in Fig. 8c. Along the habit plane of DBII, the shear strain γ_b appears, and subsequently the wall structures form in DBII (see Fig. 8d).

Zhang et al. [42] found that DBII did bear more plastic deformation than SB. In terms of the volume fraction of DBII, this deformation was roughly estimated to be $7.5 \times 10^{-3} - 2 \times 10^{-2}$. Meanwhile the intrusion and extrusion caused by DBII are stronger than those caused by SB, which is well in agreement with the formation of wall structures in DBII. Until now, the formation of wall structure in DBII has been explained well. But there is another question: Why are DBII consisting of the walls more prone to appear in [0 1 1] crystals?

For [0 1 1] or near [0 1 1] fcc single crystals, although there are four equivalent slip systems, one slip system will be always activated first during cyclic deformation; this is called the primary slip system. The activating of the primary slip system will cause latent hardening of the crystal and inhibit the initiating of the other slip systems. Li [47] pointed out that the habit planes of DBII are close to $(\bar{1}\,0\,1)$, $(0\,\bar{1}\,1)$ and $(\bar{1}\,1\,0)$, respectively. Furthermore, Li et al. [46] systematically summarized the angles between the habit planes of a variety of DB and the loading axes in different oriented copper single crystals (see Table 2). The habit plane of DBI is the same as that of SB. Accordingly, Table 2 provides such data as that, in the [0 1 1] orientation, the angle between the habit plane of SB or DBII and the loading axis has the maximum value of 60°, and the habit plane of DBII and the loading axis has the minimum value of 24°. Li et al. [46] adopted the concept of dislocation avalanche factor to explain the formation of DBII. They believed that the lattice distortion due to the tension–compression asymmetry is the main driving force forming DBII. And they also believed that DBII is more prone to appear in fcc single crystals with double- or multiple-slip orientations than with single-slip orientation.

Although [0 1 1] single crystal has four slip systems with the same Schmid factors and, in theory, the four slip systems can be activated simultaneously, no actual deformation can follow the above rule. As a rule, any crystal orientation is attributed to one of the stereographic triangles. If the triangle is surrounded by $0\,0\,1 - 0\,1\,1 - \bar{1}\,1\,1$, the primary slip system $(1\,1\,1)[\bar{1}\,0\,1]$ will be activated first. Wang et al. [48] and Wang and Laird [49] proved that, when the primary slip system operated, the slip resistance of the secondary slip system would be greatly increased because of the latent hardening. Thus, generally speaking, only at higher strain amplitudes can significant secondary SB occur; previous work [33] also proved this judgment.

For [0 1 1] single crystal, the saturation dislocation patterns are characterized by wall structure in DBII (see Fig. 6). As shown in Fig. 9a, in the stereographic triangle, no matter what kind of orientation, the angle between the orientation and $[\bar{1}\,0\,1]$ is less than that between [0 1 1] and $[\bar{1}\,0\,1]$, which is consistent with Table 2. In other words, angle ϕ between any orientation and $[\bar{1}\,0\,1]$ is not more than 60°. Thus for [0 1 1] single crystal, the ratio between the normal stress and resolved shear stress $\sigma_N^{1\,1\,1}/\tau_{SB} = \cos\phi/\cos\varphi$ is the largest among all oriented fcc crystals. According to Eqs. (3) and (4), $\tau_{DBII} = \tau_{SB}$ can be drawn, which means that the difference between σ_N and τ_{DBII} is relatively large, as shown in Fig. 9b. Thus along the slip direction $[\bar{1}\,0\,1]$ dislocations move, multiply and develop into PSB ladders. At the same time, the normal stress along [1 1 1] always imposes the action on the crystals. It can be imagined that, first, a large number of dislocations are

Table 2
Geometrical relationship between DBI, DBII and loading axis, quoted from Li et al. [46].

Loading axis	Habit plane of DBs	Angles between		
		DBI and loading axis, φ (°)	DBII and loading axis, Φ (°)	DBI and DBII (°)
[0 1 1]	DBI (0.49 0.67 0.56) DBII (−0.63 −0.18 0.76)	60	24	90
[0 3 4]	DBI (0.54 0.64 0.56) DBII (−0.59 −0.21 0.78)	56	30	89
[$\bar{2}$ 5 5]	DBI (0.70 0.57 0.50) DBII (−0.65 −0.76 0.00)	30	44	89
[$\bar{2}$ 3 3]	DBI (0.65 0.57 0.50) DBII (−0.44 −0.25 0.86)	12	35	90
[$\bar{1}$ 1 2]	DBI (0.65 0.51 0.57) DBII (−0.64 −0.07 0.77)	24	59	89
[2 2 3]	DBI (0.59 0.60 0.54) DBII (−0.64 −0.02 0.77)	23	59	88
[$\bar{1}$ 1 7]	DBI (0.65 0.60 0.46) DBII (−0.01 −0.63 0.77)	26	42	88

produced on the primary slip system, but after the regular dislocation patterns form, no more space on the primary slip system takes on the higher plastic strain. As shown in Figs. 8a and 9b, after DBII is filled with PSB whose volume fraction has reached 100% in the local region, under further combined action of the resolved shear stress τ_{SB} and the normal stress σ_N, the shearing between the original ladders is gradually replaced by mutual locking (see Fig. 8c), which leads directly to the formation of the wall structure (see Fig. 8d). The formation of the walls means that DBII will begin to shear along its habit plane. The greater the difference between σ_N and τ_{DBII}, the easier it is to form the wall structure, and the easier it is also to activate the shear plane. The shearing motion is estimated to be stronger than slip. If $\mathbf{b}_2$ is used to characterize the shear deformation, it can be seen that the Burgers vector of slip is $\mathbf{b}_1 = \sqrt{2}/2a$, and the Burgers vector of shear is $\mathbf{b}_2 = n\sqrt{3}a(n \geqslant 1)$ (see Fig. 9c). Here, slip represents the movement mode of individual dislocations, but shear aims at the movement of dislocation patterns, which is the main difference between the two deformation modes in [0 1 1] single crystal. Therefore, DBII consisting of wall structures assumes a greater plastic strain through the shearing motion in order to avoid activating the secondary slip system.

3.4. Formation mechanism of cell structure in [$\bar{1}$ 1 1] single crystal

The dislocation patterns of [$\bar{1}$ 1 1] single crystal are very different from those of [0 0 1] or [0 1 1]. Fig. 10 shows the classical dislocation patterns of [$\bar{1}$ 1 1] copper single crystal. At low strain amplitude, the dislocation patterns consist mainly of vein structures (see Fig. 10a). With increasing strain amplitude, the cell structure becomes the dominant dislocation pattern directly instead of the vein structure without the intermediate formation of PSB ladders (see Fig. 10b), which is most different from that of single-slip oriented crystal. These vein and cell structures in fatigued [$\bar{1}$ 1 1] copper single crystal have a common feature that they show more characteristics of wall structure on the observation plane (1 3 $\bar{2}$), which thus can be called "vein-wall" and "cell-wall" structure, respectively, as shown in Fig. 10c and d. But these cell walls are not the same as those wall structures on the (1 1 1) plane. From Fig. 10d, it can also be seen that the cell structures with a certain direction distribute basically along the SB. Then how do these cells form? The detailed discussion below is again from the stereographic triangle.

As shown in Fig. 4, in the stereographic triangle, the primary slip system of [$\bar{1}$ 1 1] single crystal is also activated first, followed by the operation of conjugated and coplanar secondary slip systems. Similarly, after excluding the effect of the conjugated slip system, the coplanar slip system becomes the main contribution to the formation of cell structure. The so-called coplanar slip system refers to the same slip plane with different slip directions. In the following, the second question is: How do the primary and coplanar slip systems interact with each other eventually to form the cell structure on the (1 1 1) plane?

As shown in Fig. 11a, the cell structures on the (1 1 1) plane display more anisotropy. It seems that there is no rule to follow. In the earlier discussion, it was mentioned that the orientation of [0 0 1] single crystal can be regarded as single-slip orientation fallen in one stereographic triangle because, in the actual deformation process, one primary slip system is always the first to be activated, followed by some secondary slip systems. It depends on the specific orientation of the crystal as to what kind of secondary slip system will be activated. For [$\bar{1}$ 1 1] single crystal, the easily activated secondary slip systems are the conjugated and coplanar slip systems. Also in the earlier discussion, it was made clear that activating the conjugated slip system does not change the appearance of the plateau region

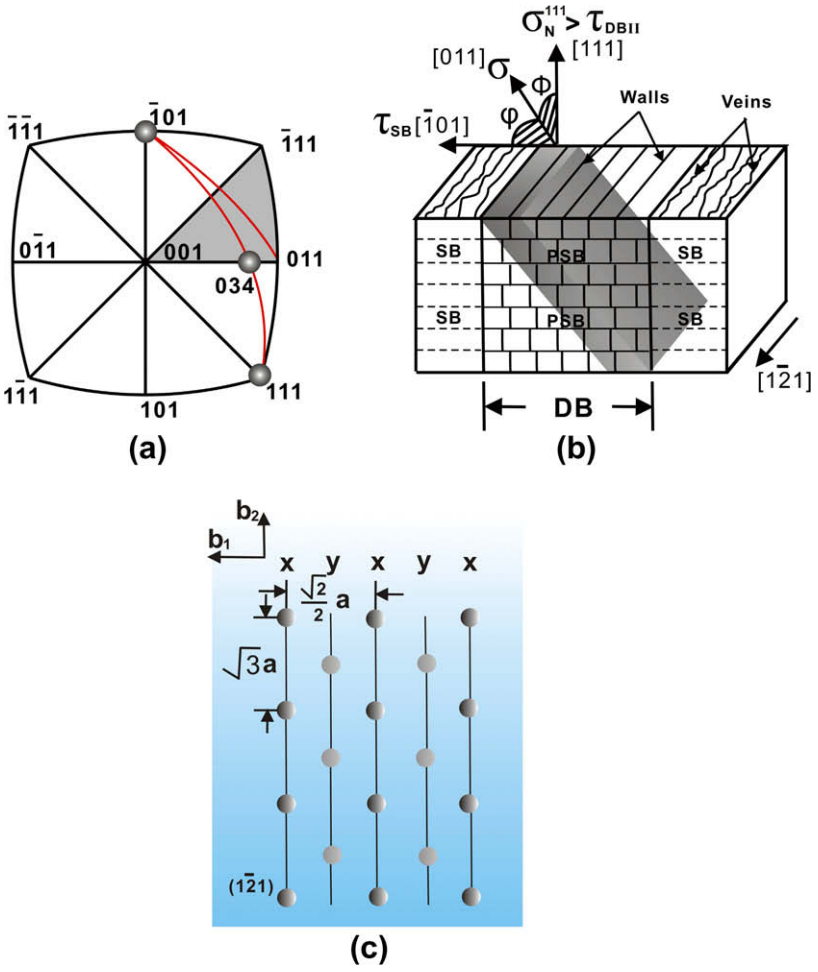

Fig. 9. Ladder-wall structure of [0 1 1] fcc single crystal: (a) relationship between loading axis, $[\bar{1}\,0\,1]$ and [1 1 1]; (b) decomposition of the axial stress σ; (c) illustration of formation of PSB wall. Viewed from $(2\,\bar{1}\,1)$ plane.

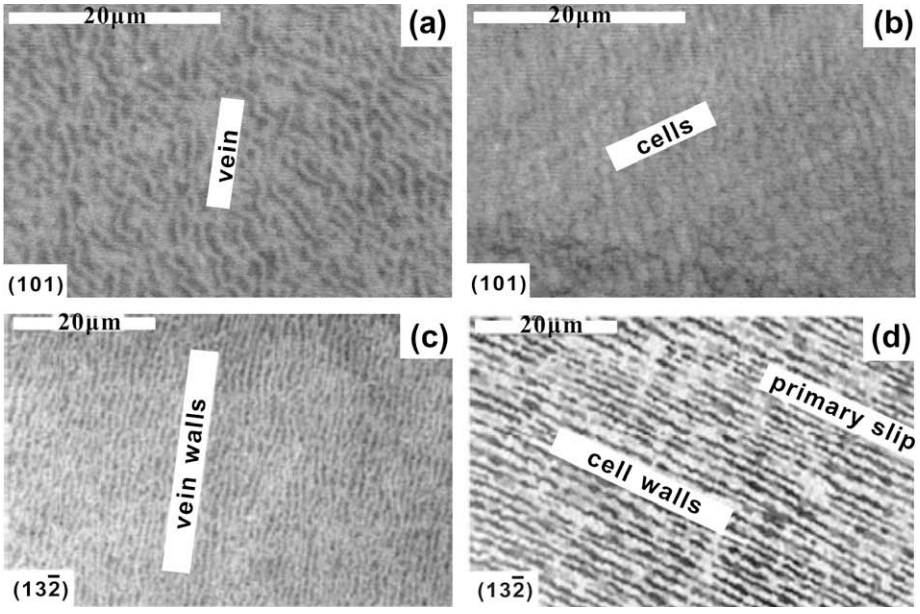

Fig. 10. Dislocation configurations of $[\bar{1}\,1\,1]$ copper single crystals at different plastic strain amplitudes: (a) $\gamma_{pl} = 1.84 \times 10^{-4}$; (b) $\gamma_{pl} = 0.92 \times 10^{-3}$; (c) and (d) $\gamma_{pl} = 4.0 \times 10^{-4}$. Quoted from Li et al. [50].

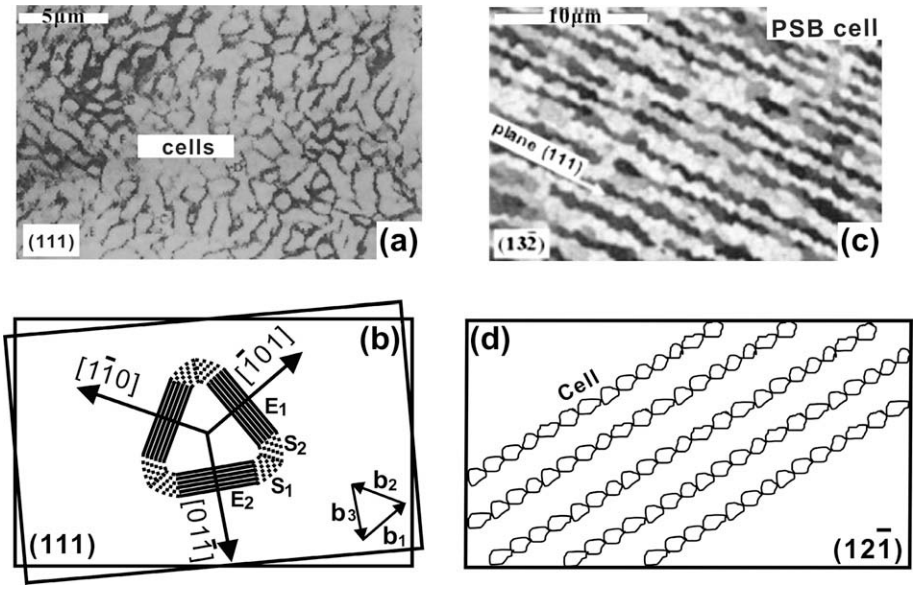

Fig. 11. Cell-wall structure of [$\bar{1}$ 1 1] fcc single crystal: (a and b) cell structure and its formation mechanism, (1 1 1) foil; (c) cell-wall structure, (1 3 $\bar{2}$) foil; (d) illustration of formation of cell-wall structure, (1 2 $\bar{1}$) foil. (a and c) quoted from Lepisto et al. [17] and Li et al. [50], respectively.

and the formation of PSB ladders. Therefore, the coplanar slip system should play the main role in the formation of cells. Fig. 4 shows that the primary and coplanar slip systems are (1 1 1)[$\bar{1}$ 0 1] and (1 1 1)[1 $\bar{1}$ 0], respectively. Jin et al. [13,14] found that the dislocations belonging to these two slip systems will form the other coplanar dislocation on the (1 1 1) plane as follows:

$$\frac{1}{2}[\bar{1}\,0\,1]+\frac{1}{2}[1\,\bar{1}\,0]=\frac{1}{2}[0\,\bar{1}\,1] \tag{5}$$

Three sets of dislocations move and proliferate on the (1 1 1) plane together, and then their corresponding PSB walls along respective slip directions are produced first (see Fig. 11b). Meanwhile, it can be seen from Fig. 11b that the reciprocating movement of edge dislocations with three Burgers vectors $\mathbf{b}_1$, $\mathbf{b}_2$ and $\mathbf{b}_3$ is equivalent to the lattice rotation with the [1 1 1] axis. It is well known that lattice rotation is coordinated by the generation of screw dislocations, which will form the twist boundary. Similarly, the screw dislocations appear along the edge of wall structures due to lattice rotation. These screw dislocations interact to form dislocation tangles such as S_1 and S_2 shown in Fig. 11b, which will connect the edge dislocation walls E_1 and E_2 into a whole. By analogy, these wall structures will further form the network structure under the action of different types of screw dislocations, which leads to the final formation of the cell structure with [1 1 1] axial rotation. Furthermore, just as the (0 1 0) plane is the best plane for the observation of the Labyrinth structure, the {1 1 1} plane can be regarded as the best plane for the observation of the cell structure. Thus, looking along the [1 2 $\bar{1}$] direction, only projection of the integrity cell structure appears on the (1 2 $\bar{1}$) plane as a result of the change of the observation plane (see Fig. 11c and d).

3.5. Intrinsic relationship between dislocation patterns and crystal orientations

Nowadays, it has been confirmed that the cyclic deformation-induced classical dislocation patterns in fcc single crystals include a two-phase structure consisting of PSB and veins mainly from single-slip orientation, the Labyrinth structure existing in the [0 0 1] orientation, the wall structure from the [0 1 1] orientation and cell structure from the [$\bar{1}$ 1 1] orientation. The questions are whether there are any intrinsic relationships between these dislocation structures and whether their appearance is by chance or by necessity.

In order to answer the above questions, the lattice structure of the fcc crystal should be considered in detail, as shown in Fig. 12a. In the lattice, there are four vectors, i.e., $\mathbf{B}_1$, $\mathbf{B}_2$, $\mathbf{B}_3$ and $\mathbf{B}_4$ in turn, according to the spaces between any atom and its surrounding atoms. It is well known that the slip system {1 1 1}⟨1 0 1⟩ of the fcc crystal corresponds to the a_1 plane and $\mathbf{B}_1$ direction in Fig. 12b, respectively. If the primary slip system is (1 1 1)[$\bar{1}$ 0 1], it will become difficult for other slip systems to activate because of latent hardening, which thus is called the latent slip system. However, plenty of experimental results have provided evidence that there could be shear systems with non-{1 1 1} planes besides the latent slip system. Of course, this does not usually happen. But under the cumulative effect of cyclic deformation, especially after the activation of the secondary slip system, the movement of dislocation patterns from the primary and secondary slip systems may be considered a complex movement, which would lead to the possible activating of the shear systems with non-{1 1 1} planes with the same effect as the dislocation reaction. Based on the above thinking, the formation of dislo-

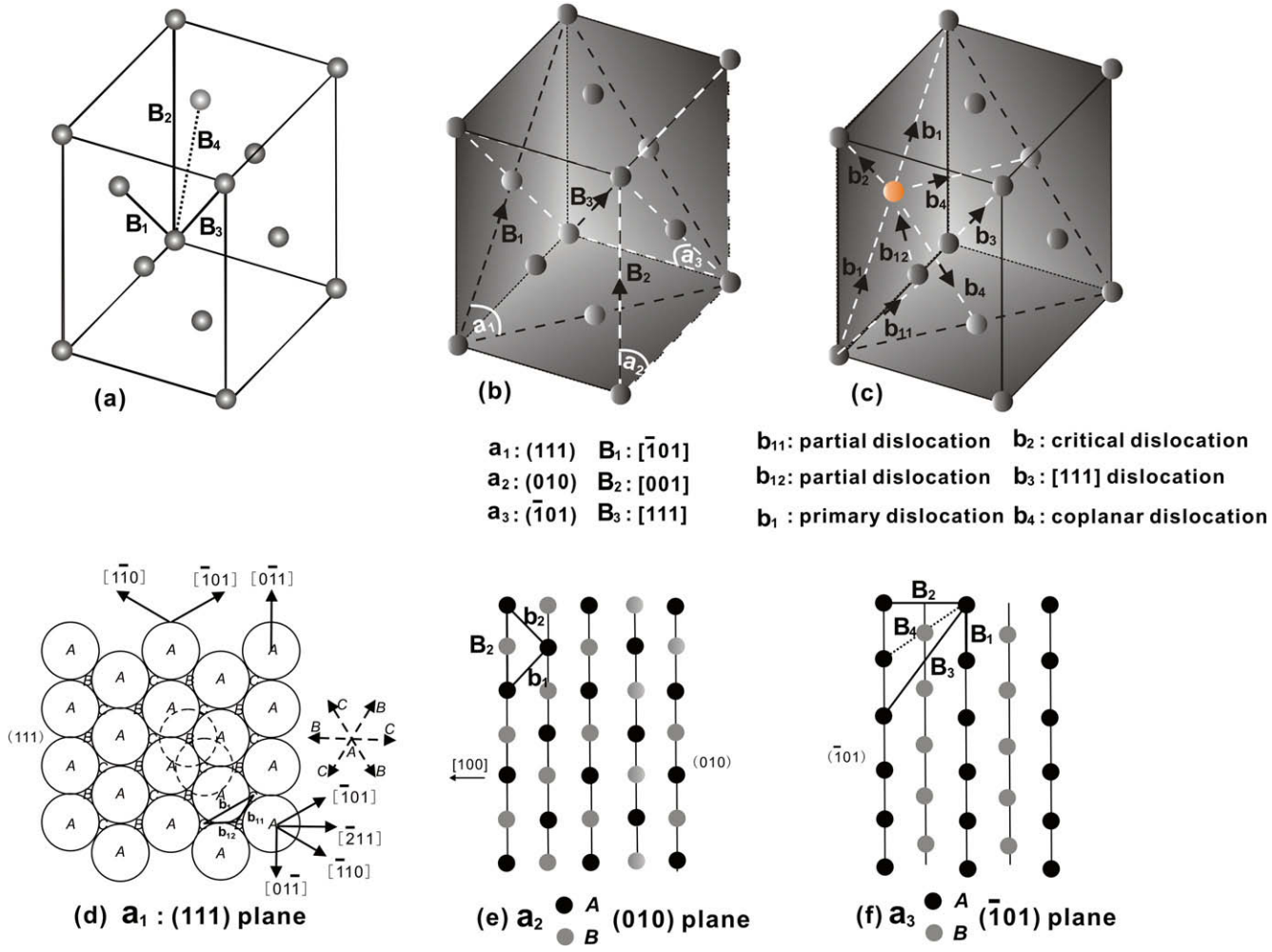

Fig. 12. Dislocation movement and selection of slip systems: (a) potential Burgers vectors; (b) slip and shear systems with three different Burgers vectors; (c) section of dislocation patterns movement; (d–f) formation of slip and shear systems.

cation patterns in the three multiple-slip oriented crystals may be explained by such simplified treatment.

Besides the latent slip systems, $a_2\mathbf{B}_2$ shown in Fig. 12b represents the latent shear system (0 1 0)[0 0 1], which corresponds to the formation of the Labyrinth structure in [0 0 1] single crystals. It is known that the Labyrinth structure results from the interaction between the primary and critical secondary slip [14]. Using the stepwise mode, the dislocation reaction can be decomposed as illustrated in Fig. 12e. In Fig. 12e, $\mathbf{b}_1$ and $\mathbf{b}_2$ represent the mappings on the (0 1 0) plane from the primary slip system $(1\,1\,1)[\bar{1}\,0\,1]$ and critical secondary slip system $(\bar{1}\,1\,1)[1\,0\,1]$, respectively. It is well known that the primary dislocation $\mathbf{b}_1$ is composed of two partial dislocations $\mathbf{b}_{11}$ and $\mathbf{b}_{12}$ (see Fig. 12d). Similarly, $\mathbf{B}_2$ can be regarded as the combination resulting from the primary dislocation $\mathbf{b}_1$ and critical dislocation $\mathbf{b}_2$. $\mathbf{b}_1$, $\mathbf{b}_2$ or $\mathbf{B}_2$ just represent the simplified form of dislocation movement. According to this thinking, the formation of the dislocation patterns in differently oriented fcc single crystals can be assumed as follows (see Fig. 12c):

(1) First, fcc single crystal by cyclic deformation starts to glide along the primary (111) slip plane and produces the prefect dislocation $\mathbf{b}_1$, consisting of two Shockley partial dislocations $\mathbf{b}_{11}$ and $\mathbf{b}_{12}$. Then, dislocations will move in the way as shown in Fig. 12c. The spontaneous motion path of these dislocations depends on the crystal orientation.

(2) If an fcc single crystal has single-slip orientation, dislocations will continue to slip back and forth along the $\mathbf{b}_1$ direction, eventually forming PSB ladder structures. In this process, slip plane a_1 is (1 1 1), the PSB ladders with the complex vector $\mathbf{B}_1$ will move along the slip direction $[\bar{1}\,0\,1]$ (see Fig. 12f), which satisfies the relations:

$$\mathbf{B}_1 = \mathbf{b}_1 = \frac{1}{2}[\bar{1}\,0\,1] = \frac{1}{6}[\bar{1}\,\bar{1}\,2] + \frac{1}{6}[\bar{2}\,1\,1] \tag{6}$$

(3) If the orientation of fcc single crystal is close to [0 0 1], as shown in Fig. 12c, activation of the critical secondary slip system makes the dislocations continue to glide along the $\mathbf{b}_2$ direction. The formation

of the Labyrinth structure is the direct result of the interaction between $\mathbf{b}_1$ and $\mathbf{b}_2$. In this process, the shear plane $a_2 = (0\,1\,0)$ will be activated, and the Labyrinth walls with the complex vector $\mathbf{B}_2$ will move along the shear direction [0 0 1] (see Fig. 12f), which satisfies the following reaction:

$$\mathbf{B}_2 = \mathbf{b}_1 + \mathbf{b}_2 = \frac{1}{2}[\bar{1}\,0\,1] + \frac{1}{2}[1\,0\,1] = [0\,0\,1] \tag{7}$$

(4) If the orientation of fcc single crystal is close to $[\bar{1}\,1\,1]$, as shown in Fig. 12c, the activation of the coplanar secondary slip system makes the dislocations continue to glide along the $\mathbf{b}_4$ direction. The interaction between $\mathbf{b}_1$ and $\mathbf{b}_4$ will contribute to the formation of the cell structure. In this process, although the slip plane is always (1 1 1), the third set of PSB ladders with the complex vector $\mathbf{B}_4$ will move along slip direction $[\bar{1}\,1\,0]$ (see Fig. 12f), which satisfies the following reaction:

$$\mathbf{B}_4 = \mathbf{b}_1 + \mathbf{b}_4 = \frac{1}{2}[\bar{1}\,0\,1] + \frac{1}{2}[0\,1\,\bar{1}] = \frac{1}{2}[\bar{1}\,1\,0] \tag{8}$$

or

$$\mathbf{B}_4 = \mathbf{b}_1 + \mathbf{b}_4 = \frac{1}{2}[\bar{1}\,0\,1] + \frac{1}{2}[\bar{1}\,1\,0] = \frac{1}{2}[\bar{2}\,1\,1] \tag{9}$$

Therefore, three sets of PSB walls with different Burgers vectors form the cell structure under the action of dislocation tangles consisting of screw dislocations.

(5) In fact, activation of the different secondary slip systems is required to carry higher plastic deformation. However, as shown in Fig. 12c, when the evenly distributed PSB on the primary slip system cannot afford higher plastic deformation, the heavily distributed PSB will first appear in local regions of the [0 1 1] crystal, which corresponds to the formation of DBII. Furthermore, in DBII the PSB ladders connect with each other into PSB walls, and the [0 1 1] crystal would rather select the shear system $a_3\mathbf{B}_3$ with a non-close-packed plane $(\bar{1}\,0\,1)$ as the effect habit system than the latent secondary slip systems. Accordingly, PSB walls with the new vector $\mathbf{B}_3$ will move along the shear direction [1 1 1], as shown in Fig. 12f. Meanwhile, the crystal deformation will also be changed from slip to shear (see Fig. 12b). The specific conversion process is as follows:

$$a_1\mathbf{B}_1 = (1\,1\,1)[\bar{1}\,0\,1] \rightarrow a_3\mathbf{B}_3 = (\bar{1}\,0\,1)[1\,1\,1] \tag{10}$$

It should be pointed out that the effect of orientation on the dislocation patterns for fcc single crystals has been far better explained. Returning to single-slip orientations, the reason for the formation of the Labyrinth or cell structures has been also made clear. The formation of complex dislocation patterns depends on the activating slip system. If the critical secondary slip system is easier to operate, the Labyrinth is more likely to be observed. If the coplanar secondary slip system is activated, the cell structure is more commonly seen. If there is no secondary slip system to be activated, the wall structure is more prone to appear. In short, for the dislocation patterns, in addition to the traditional slip systems, the shear systems with non-close-packed planes should be equally considered, which will aid better understanding of the effect of orientations on cyclic deformation behavior, especially the formation of dislocation patterns, of fcc crystals.

4. Conclusions

In order to explore the formation mechanism of dislocation patterns in differently oriented fcc single crystals, the cyclic deformation behavior of three typical multiple-slip oriented copper single crystal were summarized. Compared with the formation of the first ladder-like PSB in single-slip oriented crystals at the plastic resolved shear strain amplitude $\gamma_{pl} = 6 \times 10^{-5}$, the Labyrinth structure consisting of two dislocation walls (0 0 1) and (1 0 0) perpendicular to each other is usually found in [0 0 1] crystals. In $[\bar{1}\,1\,1]$ crystals, the cell-wall structures are the most basic dislocation pattern, and in [0 1 1] crystals, the wall structures in DBII are more prone to be observed. The habit plane of these walls is the same $(\bar{1}\,0\,1)$ plane as DBII. Based on experimental results, the dislocation patterns in fcc single crystals can be described as follows: a two-phase structure consisting of PSB and veins mainly from single-slip orientation, a Labyrinth structure existing in the [0 0 1] orientation, a wall structure from the [0 1 1] orientation and a cell structure from the $[\bar{1}\,1\,1]$ orientation. Further research shows that the formation of dislocation patterns has a direct relationship with the crystal orientation, which can be summarized as the choice of slip system. If the association between shear systems with non-close-packed planes and dislocation reactions is considered, the movement of dislocation patterns can be better understood and, subsequently, the formation principle and mechanism of more advanced dislocation patterns, including Labyrinth, cell and wall structures can be drawn.

Acknowledgements

The authors are grateful to Prof. H. Mughrabi and Prof. X.W. Li for their good suggestions and advice. Thanks are also due to H.H. Su, W. Gao, H.F. Zou and Q.Q. Duan for their assistance in the fatigue experiments and dislocation observations. This work was financially supported by the National Outstanding Young Scientist Foundation under Grant No. 50625103, the National Natural Science Foundation of China under Grant No. 50890173, and the National Basic Research Program of China under Grant No. 2010CB631006.

References

[1] Thompson N, Wadsworth N, Louat N. Philos Mag 1956;1:113.
[2] Laufer EE, Roberts WN. Philos Mag 1966;14:65.
[3] Winter AT. Philos Mag 1974;30:719.
[4] Finney JM, Laird C. Philos Mag 1975;31:339.
[5] Mughrabi H. Mater Sci Eng 1978;33:207.
[6] Helgeland O. J Inst Metals 1965;93:570.
[7] Watt DP, Embury JD, Ham RK. Philos Mag 1968;17:199.
[8] Roberts WN. Philos Mag 1969;20:675.
[9] Woods PJ. Philos Mag 1973;28:155.
[10] Mughrabi H, Herz K, Ackermann F. In: Proceedings, 4th international conference on the strength of metals and alloys, vol. 3. Nancy; 1976. p. 1244.
[11] Grosskreutz JC, Mughrabi H. Description of the work-hardened structure at low temperature in cyclic deformation. In: Argon AS, editor. Constitutive equations in plasticity. Cambridge (Mass): MIT Press; 1975. p. 251.
[12] Cheng AS, Laird C. Mater Sci Eng 1981;51:111.
[13] Jin NY. Philos Mag A 1983;48:L33.
[14] Jin NY, Winter AT. Acta Metall 1984;32:989.
[15] Jin NY. Acta Metall Sin 1988;24:299.
[16] Jin NY. Acta Metall Sin 1988;24:311.
[17] Lepisto TK, Kuokkala VT, Kettunen PO. Scr Metall 1984;18:245.
[18] Lepisto TK, Kettunen PO. Mater Sci Eng 1986;83:1.
[19] Lepisto TK, Kuokkala VT, Kettunen PO. Mater Sci Eng 1986;81:457.
[20] Gong B, Wang ZR, Wang ZG. Acta Mater 1997;45:1365.
[21] Gong B, Wang ZR, Chen DL, Wang ZG. Scr Mater 1997;37:1605.
[22] Li XW, Wang ZG, Li GY, Wu SD, Li SX. Acta Mater 1998;46:4497.
[23] Li XW, Wang ZG, Li SX. Philos Mag Lett 1999;79:715.
[24] Li XW, Wang ZG, Li SX. Philos Mag Lett 1999;79:869.
[25] Li XW, Zhang ZF, Wang ZG, Li SX, Umakoshi Y. Defect Diffus Forum 2001;188–190:153.
[26] Wang ZG, Zhang ZF, Li XW, Jia WP, Li SX. Mater Sci Eng A 2001;319–321:63.
[27] Bretschneider J, Holste C, Tippelt B. Acta Mater 1997;45:3775.
[28] Kahle E. Untersuchungen zur Stabilität bei zyklisch verformten Nickel- und Nickel–Kobalt–Einkristalle. PhD thesis, Technical University of Dresden; 1983.
[29] Buque C. Int J Fatigue 2001;23:671.
[30] Buque C, Bretschneider J, Schwab A, Holste C. Mater Sci Eng A 2001;300:254.
[31] Sastry SML, Ramaswami B, Goetz F. Metall Trans A 1976;7:243.
[32] Mughrabi H, Ackermann F, Herz K. Persistent slip bands in fatigued face-centered and body-centered cubic metals. In: Fong JT, editor. Fatigue mechanisms. ASTM STP, vol. 675. Philadelphia: ASTM; 1979. p. 69.
[33] Li P, Zhang ZF, Li SX, Wang ZG. Acta Mater 2008;56:2212.
[34] Li P, Zhang ZF, Li SX, Wang ZG. Scr Mater 2008;59:730.
[35] Li P, Zhang ZF, Li XW, Li SX, Wang ZG. Acta Mater 2009;57:4845.
[36] Zauter R, Petry F, Bayerlein M, Sommer C, Christ HJ, Mughrabi H. Philos Mag A 1992;66:425.
[37] Schwab A, Bretschneider J, Buque C, Blochwitz C, Holste C. Philos Mag Lett 1996;74:449.
[38] Melisova D, Weiss B, Stickler R. Scr Mater 1997;36:1061.
[39] Ahmed J, Wilkison AJ, Roberts SG. Philos Mag A 2001;81:1473.
[40] Zhang ZF, Wang ZG. Philos Mag Lett 1998;78:105.
[41] Zhang ZF, Wang ZG, Hu YM. Scr Mater 1999;40:1353.
[42] Zhang ZF, Wang ZG, Sun ZM. Acta Mater 2001;49:2875.
[43] Zhang ZF, Wang ZG. Acta Mater 2003;51:347.
[44] Jin NY, Winter AT. Acta Metall 1984;32:1173.
[45] Li P, Zhang ZF, Li SX, Wang ZG. Philos Mag 2009;89:2903.
[46] Li SX, Li XW, Zhang ZF, Wang ZG, Lu K. Philos Mag A 2002;82:3129.
[47] Li XW. Effect of crystallographic orientation on cyclic deformation behavior of copper single crystals. PhD thesis, Institute of Metal Research; 1998.
[48] Wang ZR, Romanow WJ, Laird C. Metall Mater Trans A 1989;20:759.
[49] Wang ZR, Laird C. Metall Mater Trans A 1989;20:2033.
[50] Li XW, Zhou Y, Guo WW, Zhang GP. Cryst Res Technol 2009;44:315.